



A new method for preform dimension and influence of relevant parameters in the gear forced throughfeed rolling process

Ziyong Ma^{1,2,3} · Lifeng Ma^{1,2} · Yuanxin Luo³ · Yongqin Wang³ · Weitao Jia^{1,2}

Received: 24 November 2019 / Accepted: 7 April 2020 / Published online: 18 April 2020
© Springer-Verlag London Ltd., part of Springer Nature 2020

Abstract

Gear rolling process is an advanced forming technology in which the rolling die extrudes the preform material to flow plastically and finally form desired gears, and the preform dimension has a decisive impact on the quality of the final formed gears. To further explore the influence of tooth-tip defects on the tooth height of the formed gears in the forced throughfeed rolling process, and ensure the quality of the formed parts, a new computational method for the preform dimension was firstly proposed. A growth coefficient model based on the effective top circle of the formed gears was also given. Then, the dependence of the effective top circle size in regard to geometric parameters and material of the formed gears such as the number of teeth, module, and pressure angle were explored by the established model and finite element analysis (FEA). Finally, the experimental results were displayed to verify the proposed computational method and theoretical model. The results show the growth coefficient increases with the increase of the number of teeth and module, and decreases as the pressure angle increases. Moreover, the material with better plastic deformation ability contributes to improving the growth coefficient. Additionally, the proposed new method and theoretical model for preform dimension calculation could be adopted in the gear rolling.

Keywords Preform dimension · Gear forced throughfeed rolling process · Growth coefficient model · FEA · Experiment

Abbreviations

α	Pressure angle of pitch circle, deg	r_{a2}^R	Actual tip radius of the formed gears, mm
α_C	Pressure angle of outside circle in which point C is located, deg	r_C	Radius of outside circle in which point C is located, mm
α_F	Pressure angle of outside circle in which point F is located, deg	r_Q	Distance between point Q and pole in the polar coordinate, mm
α_Q	Pressure angle of outside circle in which point Q is located, deg	s_r	Area of tooth-tip defects on the cross-section, mm ²
θ_Q	Angular coordinate in the polar coordinate, rad	s_t	Area between top circle and root circle on the cross-section, mm ²
r_{b2}	Base circle radius of the formed gears, mm	s_T	Area above the root circle of single tooth with considering tooth-tip defects, mm ²
r_{f2}	Root radius of the formed gears, mm	v_b	Material volume of end-flow on single tooth, mm ³
$r_{2,0}$	Initial radius of the preform, mm	B	Tooth width of the formed gears, mm
r_{a2}^E	Effective tip radius of the formed gears, mm	z_2	Number of teeth of the formed gears
		m	Module of the formed gears, mm
		K	Growth coefficient of the formed teeth
		h^*	Addendum coefficient
		c^*	Clearance coefficient

✉ Yuanxin Luo
yxluo@cqu.edu.cn

¹ School of Mechanical Engineering, Taiyuan University of Science and Technology, Taiyuan 030024, China

² Collaborative Innovation Center of Taiyuan Heavy Machinery Equipment, Taiyuan 030024, China

³ College of Mechanical Engineering, Chongqing University, Chongqing 400044, China

1 Introduction

Manufacturing of cylindrical gears in automotive transmissions is industrially mainly achieved with conventional cutting methods since these processes can ensure high-precision

of the gears [1]. Many believe that the rolling technique is only used for marking plate and shaft parts rather than forming parts with a good tooth profile. Actually, the rolling process is an excellent mass production method in plastic forming for high-strength precision gears since the gear rolling is a response to a great demand in the industry for low cost, high productivity, and pollution reduction [2]. However, there are still some challenges to be met before it is applied, such as poor tooth profile accuracy and short tool life.

Extensive research has been devoted to an improved general understanding of the gear rolling process. For instance, Neugebauer et al. [3] first described the flat die and round die rolling technique, and then proposed a method to decrease pitch error caused by a changing pitch value. Finally, the presented method improves the pitch accuracy by 50%. Ma et al. [4] studied the material flow velocity and displacement of key locations during the gear forced throughfeed rolling process through FEA, and the grid pattern was also used to track the trajectory of flowing materials in rolling experiment. Khodae and Melander [5] simulated the effects of four different combinations of die rotation direction on the rolled gear geometry with DEFORM-3D. Sasaki et al. [6] optimized the tooth profile of rolling dies and the surface rolling schedule of helical gears to obtain high-precision gears having a good tooth profile corresponding to DIN 5. Klocke et al. [7] discussed the relationship between the processing parameters and densification during the surface rolling of powder metallurgy (PM) gears by FEA. Cho et al. [8] predicted the surface densification and deformation behaviors of PM gear during the rolling process through FEA and experimental results. Marius et al. [9] introduced a device that manufactures a toothed wheel starting from a cylindrical workpiece by hot rolling process in terms of its structure and working principle. Li et al. [10] determined first the key factors affecting slippage (initial bite depth, friction coefficient, and number of teeth of rolling die) in the initial stage by FEA, and then their effects on slippage were also studied experimentally. Ma et al. [11] modeled theoretically the pitch error considering geometric relations and

process parameters in the initial stage of gear throughfeed rolling, and then the results of the proposed model were compared with those of FEA and experiments. Former investigations focus mainly on the stub-toothed gears; Landgrebe et al. [12] studied the hot roll-forming process of large gears by simulating the die design, preform design, and load demanded for rolling to explore the possibility of high-toothed gear rolling. Also, experimental trials were executed on the PWZ special machine. Fu et al. [13, 14] reported the hot rolling process of large-diameter gears by using the corresponding experiments and a finite element (FE) model coupling electromagnetic-thermal and deformation fields. Also, the heating effects of two coil structures were discussed. To increase the lifetime of the rolling dies and weaken some forming defects, Kretschmar et al. [15] recorded the contact stress and strain at the rolling die surface by an experimental setup and a staggered simulation with 2D and 3D. Wu et al. [16, 17] presented firstly a new conical gear rolling dies and the design method in the gear rolling process, then optimized the geometry of the conical gear rolling dies to prevent rabbit ear defect during the gear rolling. Finally, the optimization effect was verified by simulation and experiments. Ma et al. [18] proposed an innovative geometric design method of rolling die to reduce the forming load, root stress of dies, rabbit ear, and scratches on tooth flank. Moreover, the effects of geometric design mentioned were also analyzed by both numerical simulation and experiments.

Rabbit ear is one of the main defects in gear rolling process, and it is also the most difficult defect to be eliminated completely due to the forming principle. Therefore, with the help of FEA, Kamounh et al. [19] studied three quality issues (rabbit ear, asymmetrical flank, barreling) in the flat rolling of external helical gears and their possible solutions. Li et al. [20, 21] gave the formation mechanism of rabbit ear during the traditional radial-feed gear rolling process in terms of forming load, strain distribution, and material flow through FEA. Furthermore, the influencing factors of the rabbit ear including frictional coefficient, feeding velocity, and the number of teeth of the rolling dies were also analyzed. The reason why some

Fig. 1 Formation of rabbit ear: (a) relative sliding; (b) morphology and flow velocity

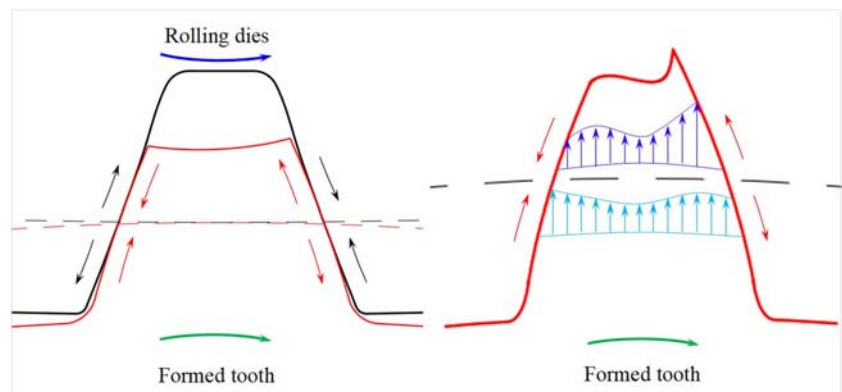
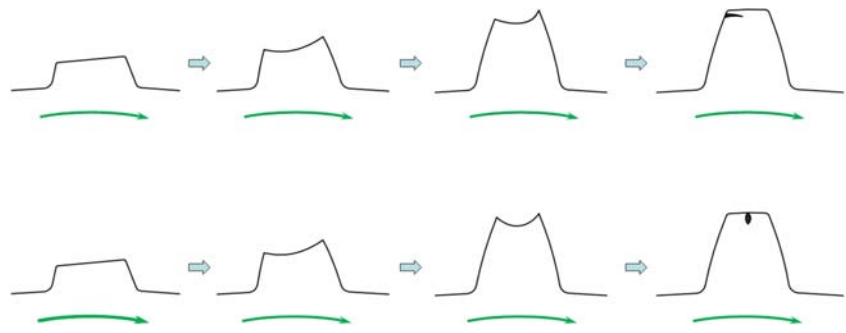


Fig. 2 Formation process of seam defect



scholars have been focused on rabbit ear is that it affects the effective tooth depth of the formed gears and the material utilization rate. In other words, the rabbit ear has a significant impact on the calculation of preform dimension in the gear rolling process.

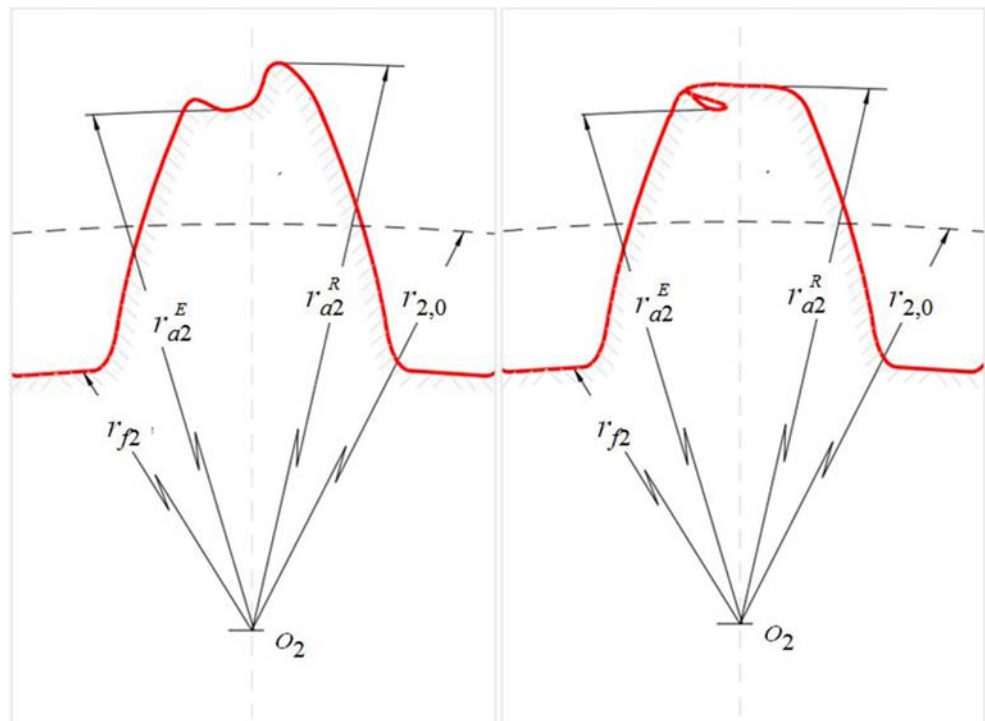
In previous research works [22-24], the preform diameter was determined by the cross-section area of the designated parts, and the influence of rabbit ear on final tip diameter of formed parts was not also taken into account. Therefore, a preliminary determination of the preform dimension in dependence of the rabbit ear effect is a crucial task for ensuring the correct dividing of the desired amount of teeth and to guarantee the tip diameter of the formed gears. This investigation aims to give a new computational method for the preform dimension and the dependence of the final tip diameter in regard to geometry and material variations of desired gears such as module, the number of teeth, and pressure angle. The rest of this study is organized as follows:

Section 2 describes the formation process of tooth-tip defects in the gear rolling process. Section 3 proposes a growth coefficient model of formed teeth with considering the effective tip diameter. Section 4 gives the FE model and results. Experimental investigations are presented in Section 5 to verify the model and FEA. Finally, the conclusions are drawn in Section 6.

2 Formation process description of tooth-tip defects

Figure 1 shows the sliding between rolling die and formed tooth in the gear rolling process. When the rolling dies and workpiece are rotated with matching gear ratio, the sliding state is shown in Fig. 1(a), which will occur on each contact tooth surface. Furthermore, friction between contact surfaces will also appear due to the existence of extrusion force, and the material on the

Fig. 3 Top circles of the formed gears



tooth surface of the formed gears will flow towards the direction of friction force caused by the rolling dies. It can be observed that the material flows from pitch circle to tooth-tip and root respectively by analyzing the relative sliding on the right flank (follower side) of the formed gears. This sliding state causes the tooth surface material near the crest of the formed gears to be pulled up by the friction force from the rolling dies. However, the sliding direction on the left flank (drive side) of the formed gears is opposite, and the surface material near the crest and root of the formed gears is observed to flow towards the pitch circle. Consequently, the morphology of the tooth profile formed by rolling is illustrated in Fig. 1(b). The sharp protrusion which appeared at the follower side of formed tooth crest is often called as rabbit ear.

As the increasing of penetration depth of rolling die teeth, the rabbit ear that appeared at the tooth crest will be compressed by the tooth bottom of the rolling dies and folded on the crest of the formed teeth. If the rolling dies rotate both clockwise and counterclockwise in the gear rolling process, the sharp protrusions will appear at both sides of the formed tooth crest. Similarly, they will also be compressed by the tooth bottom of the rolling dies and then folded on the tooth crest to form seam defect, as shown in Fig. 2.

Summarily, the tooth-tip defects of the formed gears have a significant impact on the tip diameter and quality of the final parts. To form successfully the gears with specified accuracy and dimension, it is necessary to propose a growth coefficient model of the formed teeth based on the effective top circle and analyze the influence of relevant parameters on the tip diameter,

which provides a new computational method for the preform dimension in actual production.

3 Growth coefficient model of the formed teeth

The preform dimension has no significant effect on the number of teeth of the formed parts in the gear forced rolling process that the rolling dies and preforms rotate synchronously according to the given gear ratio, and the amount of teeth depends only on the rotational speeds of rolling dies and preforms that are constant during whole rolling process. However, the preform dimension has a great influence on the tip diameter of the formed gears and load exerted on the workpiece synchronous drive system. The final tip diameter of the formed gears will be smaller than the standard value when the preform dimension is greatly less than the ideal value. If the preform dimension is larger than the ideal value, the material extruded will flow towards both ends of the preforms, and the final tip diameter will get the standard value. In this case, however, the root stress of the rolling dies may increase sharply resulting from that the space between two teeth is fully filled with the extruded material. Moreover, the load exerted on the workpiece synchronous drive system will also be increased greatly. Therefore, it is necessary to determine the preform dimension in a small range to obtain the formed gears with a standard tip diameter.

At the beginning of rolling process, the tip diameter of the formed parts increases with an increasing penetration depth of the rolling dies and rabbit ear defect appears on the tooth crest. When the sharp protrusion starts to contact the tooth bottom of

Fig. 4 Tooth profile morphology of the formed gears

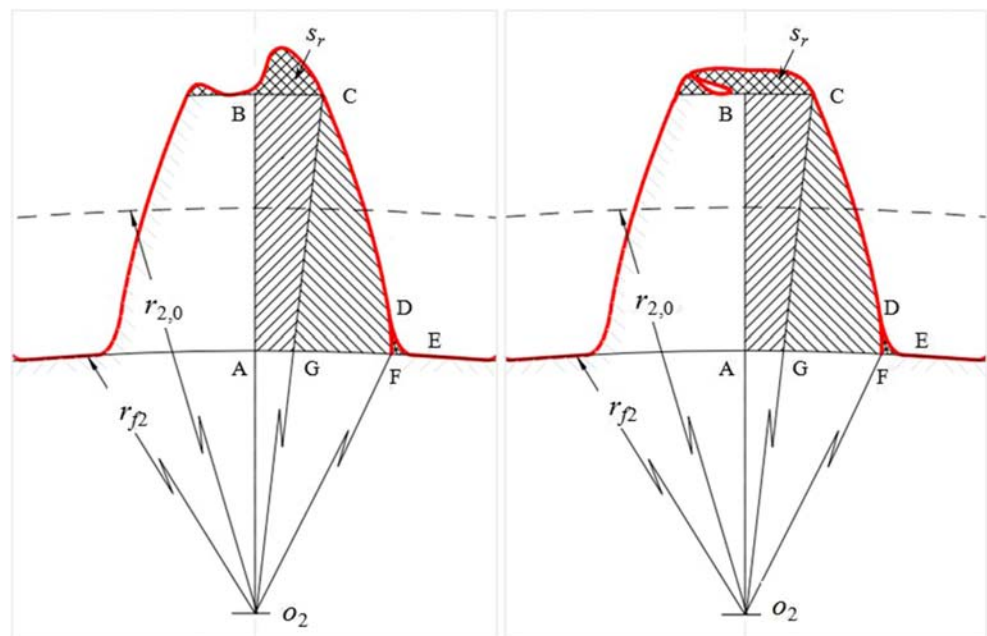


Table 1 Parameters of study cases

Cases	Rolling dies		preforms			
I-1	$z_1 = 128$	$m = 1.75 \text{ mm}$	Al6061	$m = 1.75 \text{ mm}$	$z_2 = 30$	$x_2 = 0$
I-2	$h^* = 1.0$	$\alpha = 20^\circ$		$\alpha = 20^\circ$	$z_2 = 46$	
I-3	$c^* = 0.25$				$z_2 = 62$	
II-1	$x_1 = 1.0$	$m = 1.0 \text{ mm}, \alpha = 20^\circ$	Al6061	$m = 1.0 \text{ mm}$	$z_2 = 46$	
II-2		$m = 2.5 \text{ mm}, \alpha = 20^\circ$		$m = 2.5 \text{ mm}$	$z_2 = 46$	
III-1		$m = 1.75 \text{ mm}, \alpha = 15^\circ$	Al6061	$\alpha = 15^\circ$	$z_2 = 46$	
III-2		$m = 1.75 \text{ mm}, \alpha = 25^\circ$		$\alpha = 25^\circ$	$z_2 = 46$	
IV-1		$m = 1.75 \text{ mm}$	20CrMnTi	$\alpha = 20^\circ$	$z_2 = 46$	
IV-2		$\alpha = 20^\circ$	Pb		$z_2 = 46$	

x_i is the profile shift coefficient of the rolling dies ($i = 1$) and the formed gears ($i = 2$)

the rolling dies and the penetration depth keeps increasing, the rabbit ear is transformed into the seam defect due to the compression from the tooth bottom of the rolling dies. In this situation, the outside circle of the formed gears is the actual top circle, while the outside circle located at the bottom of the seam defect is the top circle that meets the requirement of gear application. Therefore, it is named as the effective top circle in this work (see Fig. 3).

The increase of the tip diameter that resulted from the material flow should be considered to calculate the preform dimension used in the gear rolling process. In other words, the effective top circle of the formed gears after rolling should be ensured to meet the required size, assuming the effective tip radius of the formed gears is r_{a2}^E , and the actual tip radius of the formed gears is r_{a2}^R . According to the concept of addendum coefficient, the tooth height increment in radial direction of the

Fig. 5 FE model and effective top circle: **a** FE model; **b** location of the effective top circle

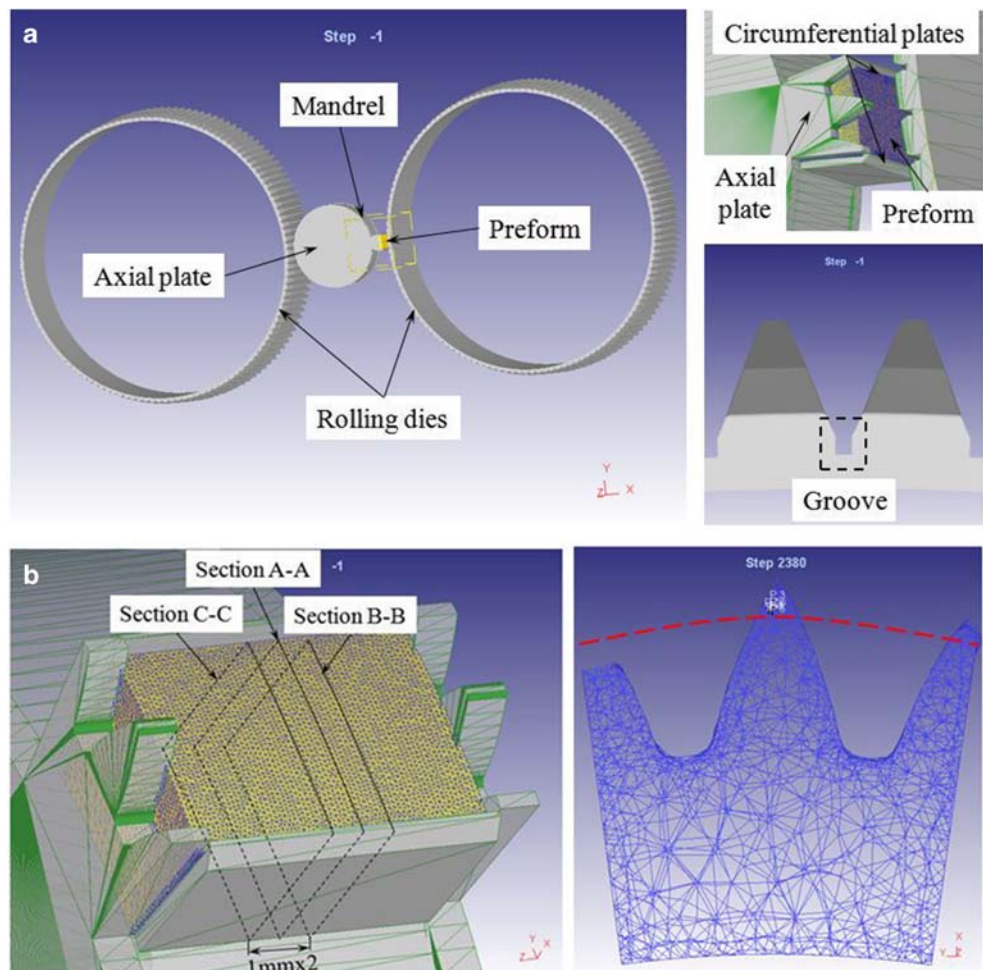
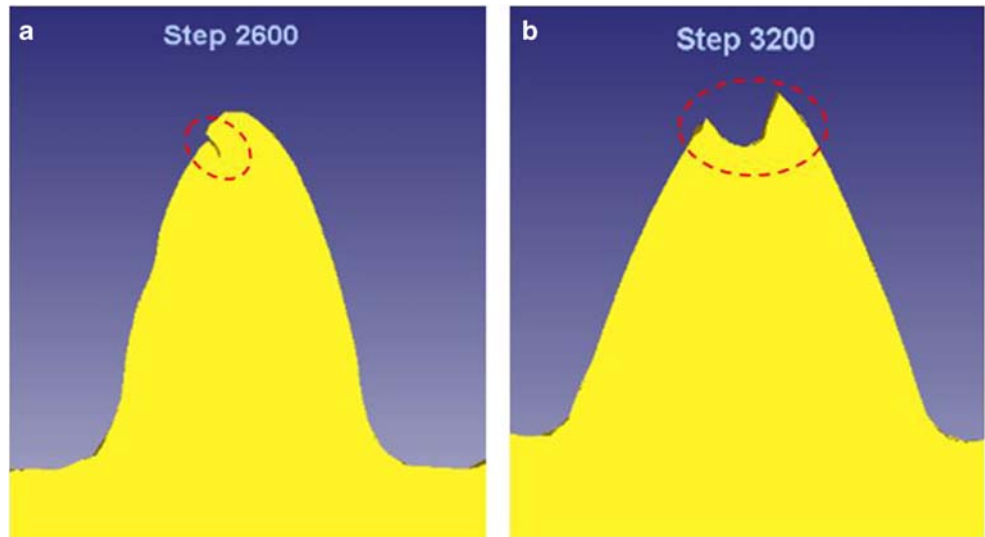


Fig. 6 Simulation results of the formed tooth crest: **a** seam defect; **b** rabbit ear



formed gears is defined as $K \cdot m$, and K is the growth coefficient of formed teeth. In this study, the calculation of preform dimension is modeled by the growth coefficient K .

$$r_{2,0} = r_{a2}^E - K \cdot m \tag{1}$$

$$K = \frac{r_{a2}^E - r_{2,0}}{m} \tag{2}$$

where $r_{2,0}$ is the initial radius of preform, mm; m is the module, mm.

Assuming that the material volume of the preform is constant during the gear rolling process, the following formula can be found:

$$\pi(r_{2,0})^2 \cdot B = \pi(r_{f2})^2 \cdot B + z_2 \cdot s_T \cdot B + z_2 \cdot v_b \tag{3}$$

where r_{f2} is the root radius of the formed gears, mm; B is the tooth width of the formed gears, mm; z_2 is the number of teeth of the formed gears; s_T is the area

above the root circle of a single tooth considering the tooth-tip defects, mm^2 ; v_b is the material volume of end-flow on a single tooth, mm^3 .

The area above the root circle of the single tooth s_T can be formulated by

$$s_T = s_t + s_r \tag{4}$$

where s_t is the area between top circle and root circle on the cross-section, mm^2 ; s_r is the area of tooth-tip defects on the cross-section, mm^2 .

Equation (3) can be rewritten as:

$$\pi(r_{2,0})^2 \cdot B = \pi(r_{f2})^2 \cdot B + z_2 \cdot (s_t + s_r) \cdot B + z_2 \cdot v_b \tag{5}$$

The tooth profile morphology of the formed gear is shown in Fig. 4, and the relevant areas are calculated with neglecting the asymmetry of the formed teeth profiles. It can be seen that the sector area is s_{ABCGA} , the area near the involute is s_{CDFGC} , and the area near the root fillet is s_{DEFD} .

$$s_t = 2(s_{ABCGA} + s_{CDFGC} + s_{DEFD}) \tag{6}$$

$$s_t = 2(s_{O_2ABCGO_2} + s_{O_2GCDFO_2} + s_{DEFD} - s_{O_2AGFO_2}) \tag{7}$$

For case 1, the sector areas $s_{O_2ABCGO_2}$ can be expressed as follows:

$$BC = \frac{\pi r_C}{2z_2} - r_C(\text{inv}\alpha_C - \text{inv}\alpha) \tag{8}$$

where r_C is the radius of outside circle in which point C is located, mm; α is the pressure angle of pitch circle, deg; α_C is the pressure angle of the outside circle in which point C is located, deg.

Table 2 Areas of the formed single tooth

Cases	s_r/mm^2	s_{DEFD}/mm^2	s_r'/mm^2	s_T/mm^2
I-1	10.8122	0.0952	0.5790	11.3912
I-2	11.4152	0.0840	0.4853	11.9005
I-3	11.3067	0.0918	0.3850	11.6917
II-1	3.6541	0.0464	0.3849	4.0390
II-2	22.7110	0.1878	1.1242	23.8352
III-1	11.0077	0.1285	0.5798	11.5875
III-2	11.2330	0.0394	0.3684	11.6014
IV-1	11.2430	0.0783	0.8650	12.1080
IV-2	11.4694	0.0951	0.4004	11.8698

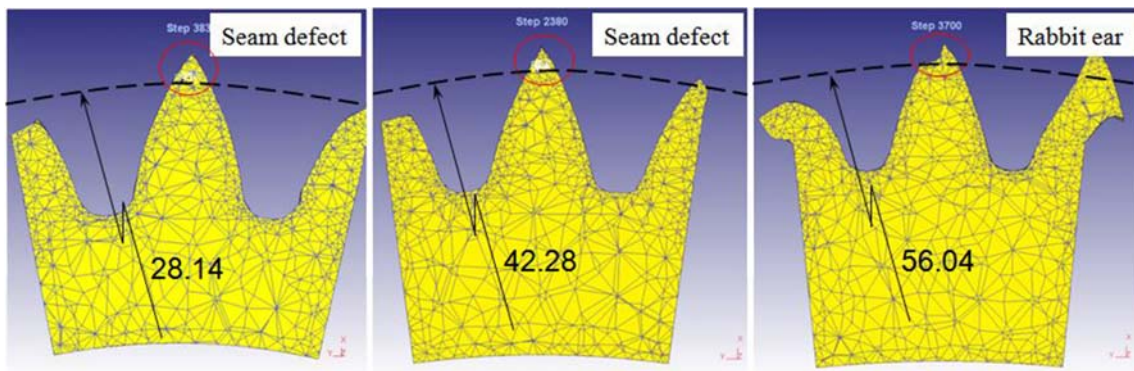


Fig. 7 Tooth-tip morphology of the formed gears with different number of teeth

$$\angle BO_2C = \frac{BC}{r_C} = \frac{\pi}{2z_2} - (inv\alpha_C - inv\alpha) \tag{9}$$

Hence,

$$s_{O_2ABCGO_2} = \frac{1}{2} r_C^2 \cdot \angle BO_2C$$

$$= \frac{r_C^2}{2} \left(\frac{\pi}{2z_2} - inv\alpha_C + inv\alpha \right) \tag{10}$$

For case 2, the area $s_{O_2GCDFO_2}$ can be expressed as follows:

The polar coordinates of point Q on the involute profile can be given by

$$\begin{cases} r_Q = r_{b2} / \cos\alpha_Q \\ \theta_Q = inv\alpha_Q = \tan\alpha_Q - \alpha_Q \end{cases} \tag{11}$$

where r_Q is the distance between point Q and pole in the polar coordinate, mm; r_{b2} is the base circle radius of the formed gears, mm; α_Q is the pressure angle of the outside circle in which point Q is located, deg; θ_Q is the angular coordinate in the polar coordinate, rad.

Hence,

$$s_{O_2GCDFO_2} = \frac{1}{2} \int_{\alpha_F}^{\alpha_C} r_Q^2 d\theta_Q = \frac{1}{2} \int_{\alpha_F}^{\alpha_C} \frac{r_{b2}^2}{\cos^2\alpha_Q} d\theta_Q$$

$$= \frac{r_{b2}^2}{6} (\tan\alpha_C^3 - \tan\alpha_F^3) \tag{12}$$

where α_F is the pressure angle of the outside circle in which point F is located, deg.

For case 3, the area $s_{O_2AGFO_2}$ can be expressed as:

$$\angle AO_2F = \frac{\pi}{2z_2} - (inv\alpha_F - inv\alpha) \tag{13}$$

$$s_{O_2AGFO_2} = \frac{1}{2} r_{f2}^2 \cdot \angle AO_2F$$

$$= \frac{r_{f2}^2}{2} \cdot \left(\frac{\pi}{2z_2} + inv\alpha - inv\alpha_F \right) \tag{14}$$

Hence, Eq. (7) can be rewritten as:

$$s_t = \frac{r_b^2}{3} (\tan\alpha_C^3 - \tan\alpha_F^3) + r_C^2 \left(\frac{\pi}{2z_2} - inv\alpha_C + inv\alpha \right) - r_{f2}^2$$

$$\left(\frac{\pi}{2z_2} + inv\alpha - inv\alpha_F \right) + 2s_{DEFD} \tag{15}$$

Also, Eq. (4) can be rewritten as:

$$s_T = \frac{r_b^2}{3} (\tan\alpha_C^3 - \tan\alpha_F^3) + r_C^2 \left(\frac{\pi}{2z_2} - inv\alpha_C + inv\alpha \right)$$

$$- r_{f2}^2 \left(\frac{\pi}{2z_2} + inv\alpha - inv\alpha_F \right) + 2s_{DEFD} + s_r \tag{16}$$

The following equation can be given by Eq. (5):

$$r_{2,0} = \sqrt{(r_{f2})^2 + \frac{z_2 \cdot s_T}{\pi} + \frac{z_2 \cdot v_b}{\pi \cdot B}} \tag{17}$$

Generally, the effective tip radius of the formed gears is the standard tip radius and defined by

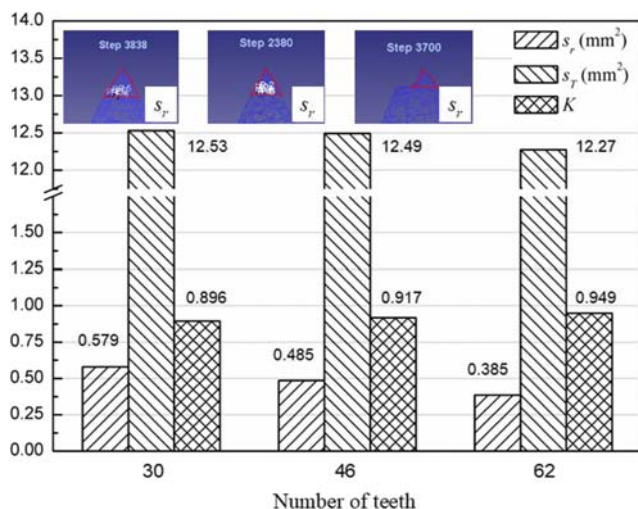


Fig. 8 Areas and growth coefficient of the formed gears with different number of teeth

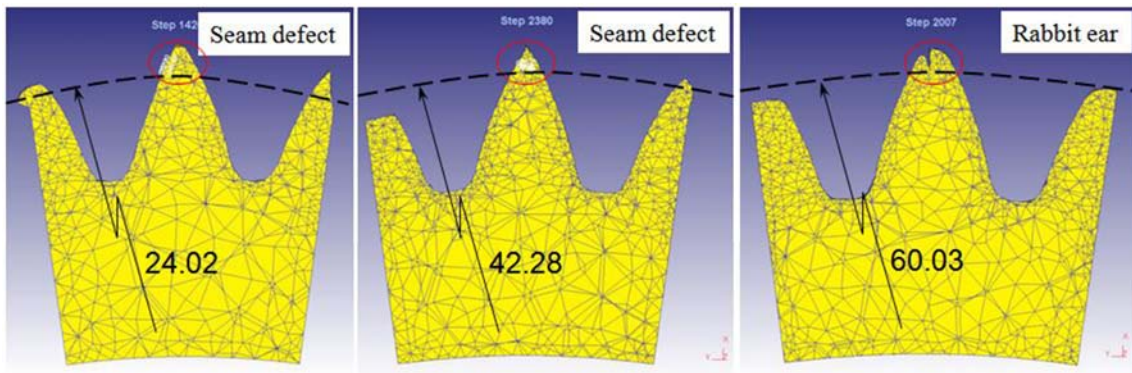


Fig. 9 Tooth-tip morphology of the formed gears with different modules

$$r_{a2}^E = \frac{m \cdot z_2}{2} + h^* \cdot m \tag{18}$$

where h^* is the addendum coefficient.

The root radius r_{f2} of the formed gears can be defined by

$$r_{f2} = \frac{m \cdot z_2}{2} - (h^* + c^*) \cdot m \tag{19}$$

where c^* is the clearance coefficient.

Substituting Eqs. (17) and (18) and (19) into Eq. (2), the growth coefficient K can be formulated by

$$K = \frac{z_2}{2} + h^* - \sqrt{\left(\frac{z_2}{2} - h^* - c^*\right)^2 + \frac{z_2 \cdot s_T}{\pi m^2} + \frac{z_2 \cdot v_b}{\pi m^2 B}} \tag{20}$$

It can be found from Eqs. (16) and (20) that the growth coefficient K varies with the number of teeth z_2 , addendum coefficient h^* , clearance coefficient c^* , module m , tooth width B , volume of material end-flow (v_b), and sectional area of single tooth profile (s_T). Meanwhile, the sectional area of the single tooth profile (s_T) is related to the pressure angle α , tooth-tip defect, and root fillet.

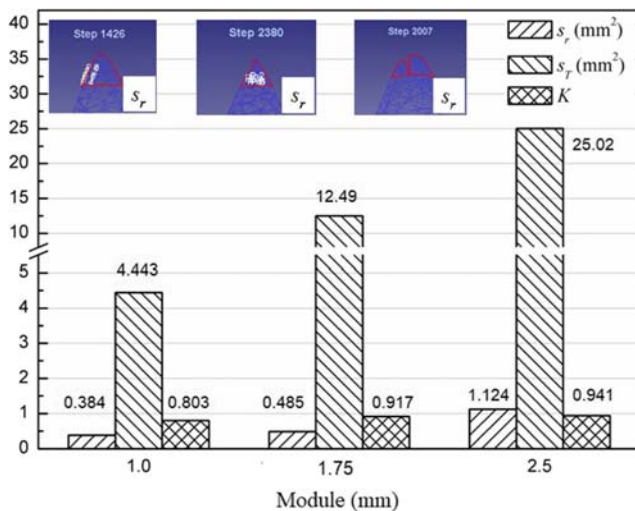


Fig. 10 Areas and growth coefficient of the formed gears with different modules

The gear throughfeed rolling process is suitable for forming a string of preforms, and the axial material flow of the remaining preforms can be neglected due to the support of surrounding materials except for the preforms at both ends of strung preforms. Therefore, the volume of material end-flow (v_b) and tooth width (B) of the remaining preforms have little effect on the growth coefficient, and Eq. (20) can be rewritten by

$$K = \frac{z_2}{2} + h^* - \sqrt{\left(\frac{z_2}{2} - h^* - c^*\right)^2 + \frac{z_2 \cdot s_T}{\pi m^2}} \tag{21}$$

4 Finite element modeling and simulation

4.1 Study cases

Generally, the addendum coefficient $h^* = 1.0$ and the clearance coefficient $c^* = 0.25$. Therefore, the finite element software DEFORM was employed to analyze the impacts of number of teeth z_2 , module m , pressure angle α , and material on the growth coefficient K in this study. The parameters of study cases are listed in Table 1.

4.2 FE modeling

4.2.1 Pre-processing

- 1) Plates were arranged in both axial and circumferential directions of the double-tooth model to prevent material from flowing along these two directions and affecting the tooth height. Furthermore, there were some grooves at the teeth bottoms of the rolling dies to contain the material of the formed teeth, which were helpful to observe the morphology development of the tooth-tip defects during the rolling process, as shown in Fig. 5 a.
- 2) The preform in the FE model was meshed into tetrahedral elements with a total number of 100,000, and the elements in a ring region near the outside surface of the preform were refined with a density ratio of 0.01. Moreover, the minimum

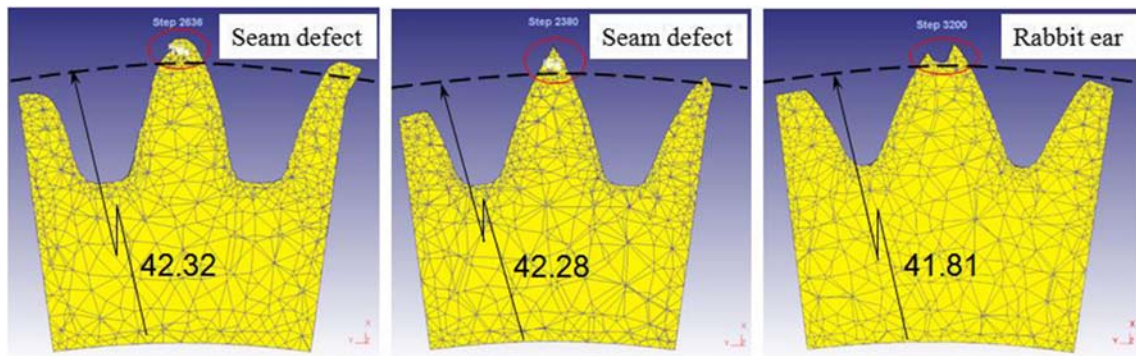


Fig. 11 Tooth-tip morphology of the formed gears with different pressure angles

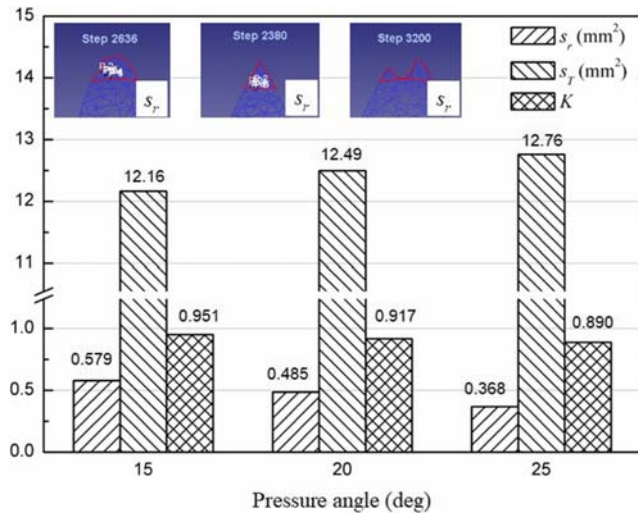


Fig. 12 Areas and growth coefficient of the formed gears with different pressure angles

element size was about 0.12 mm, and the volume compensation was applied in the simulation.

- 3) The rolling dies that were rigid body rotated on their axis and also revolved unidirectionally around the axis of the mandrel, and the rotational speed was 30 rpm and 83.4783 rpm, respectively. The rolling dies kept axial feeding at the speed of 0.7 mm/s.

- 4) The friction factor between the rolling dies and preform was set as 0.3 [25, 26], while the friction factor between the preform and baffle plates was set as 0. Moreover, the preform was fixed on the mandrel.

4.2.2 Post-processing

The areas of the tooth-tip defects (s_r) on sections A-A, B-B, and C-C were measured to calculate the growth coefficient of the formed teeth. The point tracking is used to determine the location of the tooth-tip defects and obtain the effective top circle of the formed gears to judge whether the effective tip radius reaches the standard value, as shown in Fig. 5 b.

When the FE simulation was completed, the different morphologies of the tooth-tip defects located on the formed gears were obtained, as shown in Fig. 6. The rabbit ear was transformed into the seam defect due to the severe material flow on the tooth crest of the formed gears, as shown in Fig. 6 a. However, the tooth-tip defects of some formed gears still remained as the rabbit ear, as shown in Fig. 6 b.

The figure above shows that the morphologies of the tooth-tip defects are irregular polygon whether it is the seam defect or rabbit ear defect, which makes it difficult to calculate directly s_r and s_{DEFD} with a theoretical model. Therefore, DEFORM-3D and AutoCAD were utilized to measure s_r and s_{DEFD} in this work. Firstly, point tracking in DEFORM

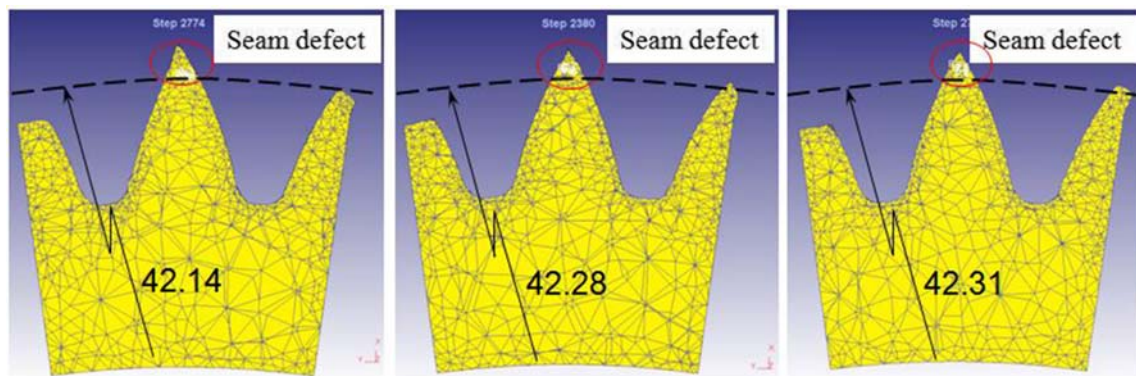


Fig. 13 Tooth-tip morphology of the formed gears with different materials

was used to get the coordinates of each point on the polygon (tooth-tip defects). Then, these coordinates were input into AutoCAD and closed by straight lines. Finally, s_r and s_{DEFD} were obtained by the area measurement function of AutoCAD. The detailed data is given in Table 2.

4.3 FE result and analysis

4.3.1 Influence of the number of formed gear teeth

It can be known from the geometric meshing theory that the gears having the same module and pressure angle as well as the different number of teeth and profile shift coefficients can be produced successfully by a pair of the rolling dies. Therefore, the impacts of the different number of the formed gear teeth on tooth-tip defect morphology were analyzed without considering the effects of other parameters, as shown in Fig. 7.

It can be seen that the actual effective tip radii (28.14 mm, 42.28 mm, 56.04 mm) of the formed gears reach the standard tip radii (28.00 mm, 42.00 mm, 56.00 mm), showing that the calculation method of the preform dimension proposed previously is quite appropriate. Moreover, the morphology of the tooth-tip defect varies as changing the number of teeth. In other words, the tooth-tip defects of the formed gears with 30 teeth and 46 teeth are the seam defect, but that of the formed gears with 62 teeth is the rabbit ear defect. While the seam defects exist authentically, they are invisible due to the mutual support of surrounding material near the tooth crest of the formed gears with 30 teeth and 46 teeth.

Two toothed plates were installed at both ends of the preform in the FE model, but they can only alleviate but not completely stop axial material flow behavior, which means that the volume of material end-flow is not negligible in the FE simulations. To ensure the consistency between the

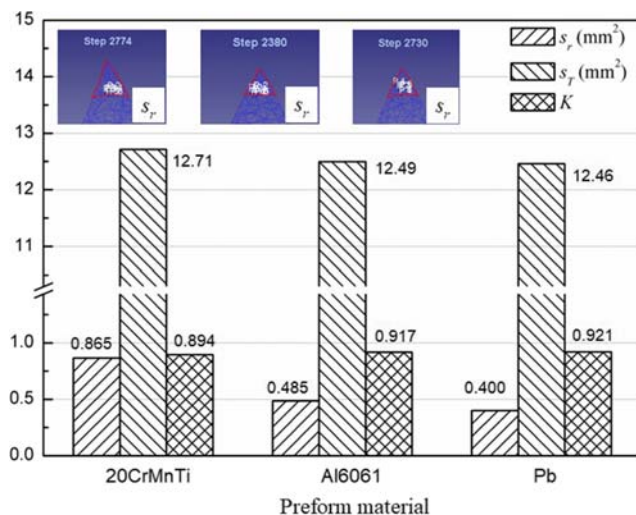


Fig. 14 Areas and growth coefficient of the formed gears with different materials

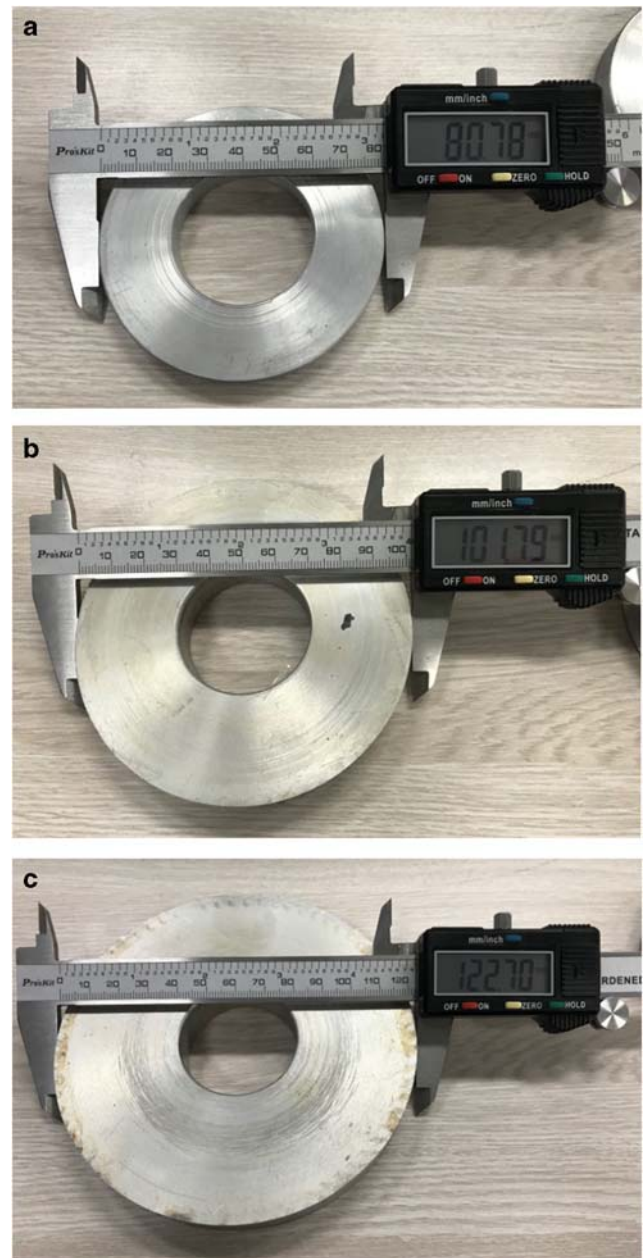


Fig. 15 Preforms with different number of teeth: **a** $z_2 = 46$; **b** $z_2 = 58$; **c** $z_2 = 70$

simulated and theoretical results, the area of the single tooth profile (s_T) calculated from the simulation results was compensated by multiplying (1.0–1.1), which is converted from the volume of the material end-flow. Variations of the areas of the tooth-tip defects (s_r), the areas of the single tooth profile (s_T), and the growth coefficient (K) are shown in Fig. 8.

As can be seen from Fig. 8, the areas of tooth-tip defects (s_r) and the area of the single tooth profile (s_T) decrease with the increasing number of teeth of the formed gears, but the growth coefficient (K) rises gradually. This variation is attributed to the larger the number of the teeth, the smaller the area of the tooth-tip defects



Fig. 16 Formed gears with different number of teeth

(s_r) and more material is ultimately used to form the tooth crest due to the less material removal in the follow-up process. Therefore, the initial dimension of preform having more teeth is smaller and the growth coefficient (K) is greater in these three given cases. It indicates that when the preform dimension is determined, the growth coefficient (K) of the formed gears with more teeth should be larger. However, it should not exceed 1 due to the volume constancy principle.

4.3.2 Influence of the module

Module is one of the key geometric parameters of gear and has a direct impact on the tooth profile of the formed gears and preform dimension, which is reflected by the fact that tooth profile of the formed gears and preform dimension increase with the increase of module. To better understand the impacts of module on the tooth-tip defect and preform dimension, three modules ($m = 1.0$ mm, 1.75 mm, 2.5 mm) were simulated and the results are shown in Fig. 9.

It can be found from Fig. 9 that the influence of module on the morphology of the formed tooth-tip is similar to that of the number of teeth mentioned in Section 4.3.1 with neglecting the impact of the number of teeth, pressure angle, and material. The tooth-tip defect of the formed gears with smaller module ($m = 1.0$ mm, 1.75 mm) is the seam defect, while that of the formed gears with larger module ($m = 2.5$ mm) is the rabbit ear defect. Also, the effective tip radii of these modules (24.02 mm, 42.28 mm, 60.03 mm) reach their standard values (24.0 mm, 42.0 mm, 60.0 mm). The influences of module on the area of the tooth-tip defects (s_r), the area of the single tooth profile (s_T), and the growth coefficient (K) are shown in Fig. 10.

By comparing the results in Fig. 10, it is found that both the area of the tooth-tip defect (s_r) and the area of the single tooth profile (s_T) increase due to the

increasing module, and the difference between s_r and s_T is that s_T rises linearly with the increase of the module, whereas s_r increases nonlinearly as the module increases, and the increment of s_r varies from 0.1004 to 0.6389 mm². This is because that the size of the formed tooth profile depends directly on the module, while there is no direct relationship between the area of the tooth-tip defect (s_r) and the module. Additionally, the growth coefficient (K) is also observed to increase with the increase of module in these given modules. This is because that the area of the tooth-tip defect (s_r) of the formed gears having a module of 1.0 mm is about 0.3849 mm², which accounts for 8.66% in the area of the single tooth profile ($s_T = 4.4429$ mm²). However, the area of the tooth-tip defect ($s_r = 1.1242$ mm²) of the formed gears having a module of 2.5 mm accounts for 4.49% in the area of the single tooth profile ($s_T = 25.027$ mm²). Therefore, the growth coefficient (K) of large module gears is greater than that of small module gears when the preform dimension is constant.

4.3.3 Influence of the pressure angle

The pressure angle of the reference circle is 20° according to the National Standard of China (GB/T1356-1988). However, 14.5°, 15°, 17.5°, 22.5°, and 25° are also often used as the pressure angle under some special conditions. To study the effect of pressure angle on the tooth-tip defect and preform dimension, three different pressure angles ($\alpha = 15^\circ$, 20°, 25°) were simulated and the results are shown in Fig. 11.

It can be observed that when the influences of the number of teeth, module, and material are neglected, the actual effective tip radius of the formed gears having a pressure angle of 15° and 20° is 42.32 mm and 42.28 mm respectively. These dimensions meet the requirement of the standard tip radius (42.00 mm), and



Fig. 17 Top circle of the formed gears with different number of teeth: **a** $z_2 = 46$; **b** $z_2 = 58$; **c** $z_2 = 70$

the tooth-tip defect is the seam defect. However, the actual effective tip radius of the formed gear having a pressure angle of 25° is 41.81 mm, which is less than the standard tip radius (42.00 mm), and the tooth-tip defect is the rabbit ear defect. This tendency is explainable because the tooth thickness at the root of the formed gear having a pressure angle of 25° is larger than those of the formed gears having a pressure angle of 15° and 20° . Therefore, the material volume used for tooth height increment decreases, and finally the effective tip radius of the formed gear having a pressure

angle of 25° does not reach the standard size. The influences of the pressure angle on the area of the tooth-tip defects (s_r), the area of the single tooth profile (s_T), and the growth coefficient (K) are shown in Fig. 12.

It is seen that the area of the single tooth profile (s_T) increases with the increase of the pressure angle in the range of 15° to 25° , whereas the area of the tooth-tip defects (s_r) and the growth coefficient (K) decrease as the pressure angle rises in this given range. The reason for this variation is that the material at the root of the formed gear having the pressure angle of 25° is greater than those of the formed gears having the pressure angles of 15° and 20° , and the material volume used for tooth height increment of the formed gear having the pressure angle of 25° decreases, resulting in the reduction of the area of tooth-tip defects (s_r). Meanwhile, the effective tip radius of the formed gear with a pressure angle of 25° is not up to the standard size. Therefore, the initial preform dimension needs to be increased and the growth coefficient (K) should be reduced.

4.3.4 Influence of the material

As mentioned in the previous analysis, the material flow velocity gradient over the cross-section is the root cause of the end-flow effect, rabbit ear, and asymmetric flank. The material flow behavior is determined by the properties of the material. To analyze the effect of the material on the tooth-tip defect and preform dimension, three different materials (20CrMnTi, Al6061, and Pb) were used in this section. The tooth-tip morphologies of different materials are shown in Fig. 13.

By analyzing the simulation results, it is seen that all the actual effective tip radii (42.14 mm, 42.28 mm, and 42.31 mm) of the three materials reach the dimension requirement of the standard tip radius (42.00 mm). Additionally, the better the plastic deformation ability of the material, the greater the actual effective tip radius becomes. This is due to the fact that the flow uniformity of material with excellent plastic deformation ability is better, and the material volume used for forming the tooth-tip defect is less. Therefore, the better the plastic deformation ability of the material, the greater the actual effective tip radius of the formed gear becomes. The tooth-tip defects of the three materials are the seam defects.

Figure 14 compares the area of the tooth-tip defects (s_r), the area of the single tooth profile (s_T), and the growth coefficient (K) in three materials (20CrMnTi, Al6061, and Pb); it is found that the area of the single tooth profile (s_T) of Al6061 is quite close to that of Pb, while the area of the single tooth profile (s_T) of 20CrMnTi is larger than that of Al6061 and Pb. The areas of the single tooth profile (s_T) in the three materials should be the same according to the constancy of volume. The reason for this phenomenon is

believed to be the error in data acquisition and the difference in material flow properties. Additionally, it is also seen that the area of the tooth-tip defects (s_r) of 20CrMnTi is 0.865 mm^2 and larger than that of Al6061 and Pb (0.4853 mm^2 and 0.4004 mm^2), which is mainly associated that the plastic deformation ability of 20CrMnTi is worse than that of the other two (Al6061 and Pb). Moreover, the growth coefficient (K) of 20CrMnTi is smaller than that of Al6061 and Pb due to the area of the tooth-tip defects (s_r).

Summarily, the influences of the number of teeth, module, pressure angle, and material on the area of the tooth-tip defects (s_r), the area of the single tooth profile (s_T), and the growth coefficient (K) are analyzed by using FE software DEFORM. The variation law of the growth coefficient (K) under different conditions is obtained, and the initial dimension of the preform can be determined by combining the interpolation method and Eq. (1).

5 Experimental investigation

5.1 Experimental procedure

5.1.1 Preform preparation

The growth coefficients of the formed gears with 30 teeth, 46 teeth, and 62 teeth in FE simulations were first fitted linearly, and then a fitting equation with the number of teeth of the formed gears as an independent variable was obtained. Finally, the growth coefficients of the formed gears with 46 teeth, 58 teeth, and 70 teeth in experiments were calculated according to the fitting equation, which were 0.9174, 0.9409, and 0.9649, respectively. Moreover, the initial radii of the preform with

46 teeth, 58 teeth, and 70 teeth were determined by Eq. (1). The calculation results were 40.39 mm, 50.85 mm, and 61.31 mm, respectively. The preforms (Al6061) with three dimensions were prepared by machining, as shown in Fig. 15.

5.1.2 Experimental settings

Five preforms were first strung together by a mandrel and fastened by locking block and nut, and then the preforms string was clamped by the clampers along the axis of axial infeed cylinder to execute the rolling experiments. The parameters of rolling equipment during the experimental process were set as follows: the rotational speed of rolling dies is 20 rpm, the axial infeed speed of preforms was 0.7 mm/s, and oil lubrication was adopted [25]. Finally, the formed gears are shown in Fig. 16.

5.2 Experimental result and analysis

The inhomogeneous flow of preform material in the rolling process results in the rabbit ear defect that appeared at the tooth crest, which will affect the measuring accuracy of the tip radius of the formed gears. Therefore, a digital vernier caliper was used to measure the tip radius in this work, and the specific steps are as follows:

- (1) The number of teeth of these preforms was even, and theoretically the two teeth with an angle difference of 180° were on a straight line passing through the center of a circle. Therefore, $(z_2/6 + 1)$ pairs of teeth were marked by a red pen at intervals of three teeth (see Fig. 17).

Table 3 Actual tip diameter of the formed gears

Preform case	46		58		70	
1	84.10	84.11 ± 0.032	105.14	105.144 ± 0.036	126.20	126.158 ± 0.050
2	84.06	<i>(84.00)</i>	105.16	<i>(105.00)</i>	126.22	<i>(126.00)</i>
3	84.14		105.10		126.14	
4	84.12		105.08		126.20	
5	84.16		105.12		126.22	
6	84.12		105.16		126.12	
7	84.08		105.20		126.10	
8	84.10		105.18		126.16	
9			105.16		126.10	
10			105.14		126.22	
11					126.10	
12					126.12	

Italics in brackets are the standard tip diameters

- (2) The distances between the lowest points of each pair of teeth crests were measured by the digital vernier caliper and recorded in Table 3.
- (3) The data recorded in Table 3 were averaged and the mean values of tip radii of the formed gears ($z_2 = 46, 58, \text{ and } 70$) were also obtained.

It can be seen from Table 3 that the mean values of the tip diameters of three formed gears ($z_2 = 46, 58, \text{ and } 70$) are larger than their standard tip diameters. This phenomenon is related to the fact that the proposed new method for calculating the preform dimension based on the effective top circle can be used in industrial production, and the FEA results are also relatively reliable.

6 Conclusions

The formation process of the tooth-tip defects and new calculation method for preform dimension as well as the influencing factors of formed tooth depth in the gear forced throughfeed rolling process are investigated in this paper, and the impacts of relevant parameters on the effective top circle of the formed gears are analyzed through case study and FE model. Also, the new method for calculating the preform dimension is verified by the experiment. The following conclusions are drawn:

- 1) Rabbit ear and seam defects depending on the penetration depth of the rolling dies appear on the tooth crest of the formed gears, and they resulted from material flow velocity gradient and are affected by sliding and friction.
- 2) The proposed growth coefficient model of the formed teeth can well reveal the influences of geometry such as module, number of teeth, and pressure angle on the final tip diameter of the formed gears. It will also be applicable for predicting the preform dimension in the gear rolling process.
- 3) It can be identified by theoretical and FEA results that the growth coefficient increases as the number of teeth and module increase and decreases with the increase of pressure angle. The reason for this variation is believed to be the difference in the area of the tooth-tip defects and the area of a single tooth profile.
- 4) The material with better plastic deformation ability is beneficial to increase the growth coefficient. Moreover, the proposed new method for the preform dimension is also verified by the experiments and could be adopted in industrial production.

Funding information This project is supported by the National Natural Science Foundation of China (No. 51775062), Shanxi Province Science Foundation for Youths (No. 201901D211292), and Initial Scientific Research Foundation of Taiyuan University of Science and Technology (No. 20192022).

References

1. Kramer P, Groche P (2018) Defect detection in thread rolling processes -experimental study and numerical investigation of driving parameters [J]. *Int J Mach Tools Manuf* 129:27-36. <https://doi.org/10.1016/j.ijmactools.2018.02004>
2. Takemasu T, Shinbutsu T (2014). Form rolling for finishing powder metal gears [J]. *Gear Solutions, Media Solutions, Inc:* 33-39
3. Neugebauer R, Putz M, Hellfritsch U (2007) Improved process design and quality for gear manufacturing with flat and round rolling [J]. *Ann CIRP* 56(1):307-312. <https://doi.org/10.1016/j.cirp.2007.05.071>
4. Ma ZY, Luo YX, Wang YQ, Willens DC (2019) Numerical and experimental investigation on material flow in gear forced throughfeed rolling process [J]. *Int J Adv Manuf Technol* 104: 3361-3381. <https://doi.org/10.1007/s00170-019-03895-9>
5. Khodae A, Melander A (2014) A study of the effects of reversal cycle in the gear rolling process by using finite element simulations [J]. *Key Eng Mater* 611-612(3):134-141. <https://doi.org/10.4028/www.scientific.net/kem.611-612.134>
6. Sasaki H, Shinbutsu T, Amano S, Takemasu T, Sugimoto S, Koide T, Nishida S (2014) Three-dimensional complex tooth profile generated by surface rolling of sintered steel helical gears using special CNC form rolling machine [J]. *Prod Eng* 81:316-321. <https://doi.org/10.1016/j.proeng.2014.09.170>
7. Klocke F, Schroder T, Kauffmann P (2007) Fundamental study of surface densification of PM gears by rolling using FE analysis [J]. *Prod Eng* 1(2):113-120. <https://doi.org/10.1007/s11740-007-0006-z>
8. Cho H, Shin Y, Hwang SW, Gu JH, Baek JH (2015) Finite element simulation of PM gear rolling process [J]. *Powder Metall* 58(3): 202-208. <https://doi.org/10.1179/1743290115Y.0000000011>
9. Marius T, Dana-Adriana IV, Alabanda OR, Monica SBI (2019) A device for gear fabrication by hot rolling on presses [J]. *Prod Manuf* 32:59-67. <https://doi.org/10.1016/j.promfg.2019.02.183>
10. Li J, Wang GC, Wu T (2016) Numerical simulation and experimental study of slippage in gear rolling [J]. *J Mater Process Technol* 234:280-289. <https://doi.org/10.1016/j.jmatprotec.2016.03.030>
11. Ma ZY, Luo YX, Wang YQ (2018) On the pitch error in the initial stage of gear roll-forming with axial-infeed [J]. *J Mater Process Technol* 252:659-672. <https://doi.org/10.1016/j.jmatprotec.2017.10.023>
12. Landgrebe D, Sterzing A, Lahl M, Druwe T, Taubert AM (2017) Hot rolling of large gears [J]. *Open Access Library J* 4:e3152. <https://doi.org/10.4236/oalib1103152>
13. Fu XB, Wang BY, Zhu XX, Tang XF, Ji HC (2017) Numerical and experimental investigations on large-diameter gear rolling with local induction heating process [J]. *Int J Adv Manuf Technol* 91(1-4): 1-11. <https://doi.org/10.1007/s00170-016-9713-y>
14. Fu XB, Wang BY, Tang XF, Ji HC, Zhu XX (2017) Study on induction heating of workpiece before gear rolling process with different coil structures [J]. *Appl Therm Eng* 114:1-9. <https://doi.org/10.1016/j.applthermaleng.2016.11192>
15. Kretzschmar J, Stockmann M, Hellman J, Schiller S, Hellfritsch U (2015) Experimental-numerical investigation of the rolling process of high gears [J]. *Exp Tech* 39:28-36. <https://doi.org/10.1111/ext.12016>
16. Wu T, Wang GC, Li J, Yan K (2018) Investigation on gear rolling process using conical gear rollers and design method of the conical gear roller [J]. *J Mater Process Technol* 259:141-149. <https://doi.org/10.1016/j.jmatprotec.2018.04.034>
17. Wu T, Wang GC, Li J, Yan K (2019) Structure design and effects of conical gear roller on restraining rabbit ear defects during gear rolling [J]. *Int J Adv Manuf Technol* 103:1621-1631. <https://doi.org/10.1007/s00170-019-03730-1>

18. Ma ZY, Luo YX, Wang YQ (2018) Geometric design of the rolling tool for gear roll-forming process with axial-infeed [J]. *J Mater Process Technol* 258:67-79. <https://doi.org/10.1016/j.jmatprotec.2018.03.006>
19. Kamouneh AA, Ni J, Stephenson D, Vriesen R, DeGrace G (2007) Diagnosis of involutometric issues in flat rolling of external helical gears through the use of finite-element models. *Int J Mach Tools Manuf* 47:1257-1262. <https://doi.org/10.1016/j.ijmachtools.2006.08.015>
20. Li J, Wang GC, Wu T (2017) Numerical-experimental investigation on the rabbit ear formation mechanism in gear rolling [J]. *Int J Adv Manuf Technol* 91(9-12):3551-3559. <https://doi.org/10.1007/s00170-017-0009-7>
21. Li J, Wang GC, Wu T (2018) Effect of process factors on the rabbit ear based on numerical simulation and experimental study in gear rolling [J]. *Int J Adv Manuf Technol* 94(9-12):4055-4064. <https://doi.org/10.1007/s00170-017-1092-5>
22. Zhang DW, Zhao SD (2014) New method for forming shaft having thread and spline by rolling with round dies [J]. *Int J Adv Manuf Technol* 70:1455-1462. <https://doi.org/10.1007/s00170-013-5387-x>
23. Wang ZK, Zhang Q (2008) Numerical simulation of involutes spline shaft in cold rolling forming [J]. *J Cent S Univ Technol* 15(s2):278-283. <https://doi.org/10.1007/s11771-008-0471-3>
24. Cui MC, Zhao SD, Zhang DW, Chen C, Li YY (2017) Finite element analysis on axial-pushed incremental warm rolling process of spline shaft with 42CrMo steel and relevant improvement. *Int J Adv Manuf Technol* 90:2477-2490. <https://doi.org/10.1007/s00170-016-9566-4>
25. Khodae A (2015) Gear rolling for production of high gears [D]. KTH Royal Institute of Technology, Stockholm
26. Neugebauer R, Hellfritsch U, Lahl M, Schiller S, Milbrandt M (2011) Innovations in rolling process of helical gears [J]. *AIP Conf Proc* 1315:569-574. <https://doi.org/10.1063/1.3552507>

Publisher's note Springer Nature remains neutral with regard to jurisdictional claims in published maps and institutional affiliations.